Evaluation of Electric Field Distributions in a Car

Kunihiko Yamada[1], Satoru Horiuchi[1], Shingo Tanaka[1], Yoshihide Yamada[2], Naobumi Michishita[3]
[1] *Yazaki Research and Technology Center (YTC), Yazaki Corporation ,*
3-1 Hikari-no-oka, Yokosuka, Kanagawa, 239-0847 Japan, ku-yamada@ytc.yzk.co.jp
[2] *Electrical and Electronic Engineering Department, National Defense Academy*
1-10-20 Hashirimizu, Yokosuka, Kanagawa, 239-8686 Japan, yyamada@cc.nda.ac.jp
[3] *Electrical Engineering Department, University of California, Los Angeles*
CA, 90095, USA, naobumi@ee.ucla.edu

Abstract

Evaluation of electric fields inside and outside a car is strongly needed, when wireless communication systems are employed in a car. In this paper, electric field distributions in a car are clarified through calculations and measurements. A 1/3 scale down model is employed. Used frequency is 2859MHz that is 3 times of 953MHz. An optical electric field probe is employed in measurements so as to minimize disturbances caused by a metallic feed cable. By a method of moment simulator utilizing the multilevel fast multipole method scheme, calculations are performed on a personal computer. This scheme achieves lightning of calculation times and memories. In comparisons of measured and simulated results, very good agreements are achieved. As a result, accuracies of measured and calculated results are ensured.

1. INTRODUCTION

Recently, radio communication systems being applied inside cars are increasing rapidly [1-2]. So, evaluation of electric fields inside and outside a car is strongly needed in order to optimize locations of radio equipments.

Previously, some research attempts were made. Electric field distributions were analysed through a resonance theory of rectangular box [3]. Simulation examples of electric fields inside a car through FDTD [4] and radiations from antennas inside a car [5] were made. However, exact comparisons of calculated and measured electric field distributions were not made. The main reason is considered that precise measurements of electric fields were quite difficult.

In this paper, precise measurement is attempted by employing an optical electric field probe. A 1/3 scale down model car is used. Applied frequency is 2859MHz which corresponds to 953MHz at a real size car. Simulations are conducted by a method of moment (MoM) simulator equipped a multilevel fast multipole method (MLFMM) scheme. This simulator can save computer memory so much and speed up calculation time. Finally, exact comparisons of calculated and measured results are made.

2. A NUMERICAL EVALUATION TOOL

A simulated car model is shown in Fig.1. This car model is a 1/3 scale down size of a middle-class sedan. A microstrip antenna (MSA) is used as a radiator and installed at the center of the dashboard. Electric field distributions inside a car are simulated by a MoM simulator (FEKO) [6]. Simulation conditions are summarized in Table I. This simulator can utilize a MLFMM and can save calculation time and memory. The car body is composed of small segments of 1/7 wavelength (λ). The MSA is composed of 1/15 wavelength segments. The number of unknown currents to be calculated is 47,774. It is shown that calculation matrix elements and memory capacity are reduced to 1/100 and 1/50 by MLFMM scheme.

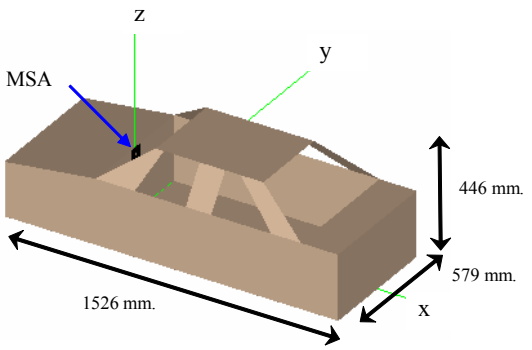

Fig. 1: Simulation model..

Table I Simulation conditions

PC spec.	Clock time	3.2 GHz
	Memory	2G Byte
	OS	Windows XP professional
EM sim.	Method	MoM with MLFMM
	Frequency	2859MHz
	Segment/λ	1/7(car model),1/15(MSA)
	Unknown currents	47,774
	Matrix elements	21,041,370 (2,282,450,624 w/o MLFMM)
	Memory requirement	773Mbyte (34,825Mbyte w/o MLFMM)
	Calculation time	1.7 hours (cannot calc. w/o MLFMM)

3. ELECTRIC FIELDS MEASUREMENT TOOL

An optical electric field probe system is shown in Fig.2 . A non metallic probe and an optical fiber cable are inserted in a

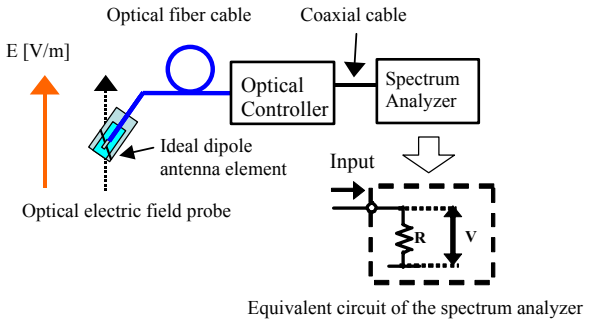

Fig. 2: Optical electric field probe system.

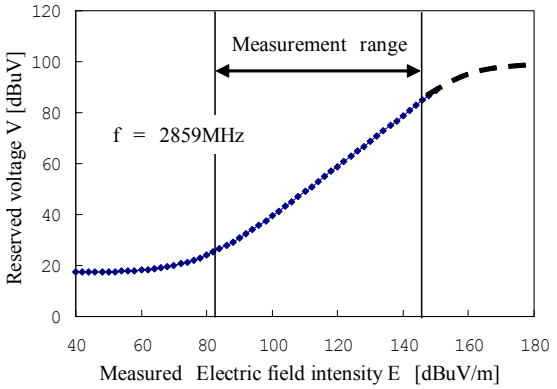

Fig. 3: Received voltage vs. electric field of a optical electric field probe.

measurement region. So, electric fields are not disturbed absolutely. The measured electric filed (E) is calculated from the measured voltage (V) through the next equation.

$$E[dBV/m] = AF[dB/m] + V[dBV] \quad \cdots\cdots (1)$$

Here, AF is called an antenna factor. Fig.3 shows a calibration curve of E and V. AF corresponds to a conversion coefficient of E to V. In this case, AF becomes 61.2dB/m.

4. Experimental Setup

An experimental setup of electric field measurements in a car is shown in Fig.4. The scale model is fabricated of aluminium panels with 1mm thickness. MSA is fed by an oscillator in the bonnet, with 1mW output power. The feed cable to MSA runs through a small hole in order to reduce radiation from a cable. An optical electric field probe is set on the top of a styrene foam block and is moved in a x-y plane. An optical electric field probe and an optical cable are non metallic materials. Electric fields inside a car are not disturbed absolutely. The signal from an optical controller is received by a spectrum analyzer, and is converted to electric field by Eq.(1). Measured and simulated radiation patterns of the MSA are shown in Fig.5. In E and H planes, measured and simulated results agree well. The measured antenna gain is 4.6 dBi.

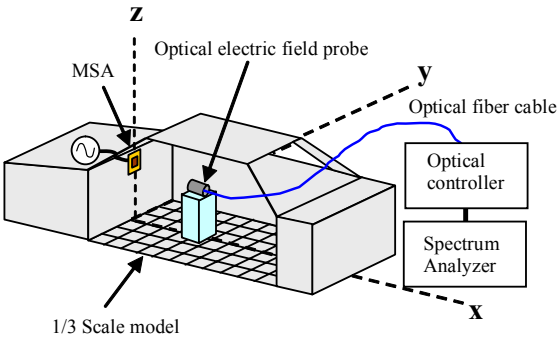

Fig. 4: An experimental setup.

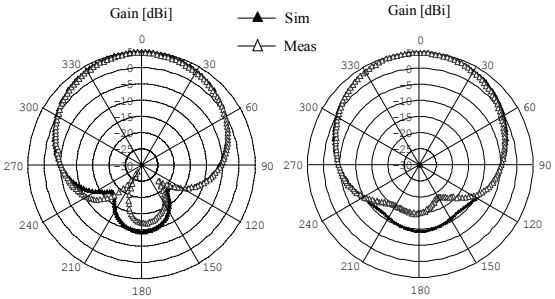

(a) θ plane (b) φ plane

Fig. 5: Radiation patterns of the MSA.

5. Measured and Simulated Results

A. *Horizontal Polarization*

Fig.6 shows electric fields in front of the MSA along the x axis, with distance step=10mm(≈λ/10). Measurements are conducted in a horizontal polarization. A standing wave shape of electric field is observed due to multi-reflection in a car. In the region of d<0.1m, direct radiations from the MSA are dominant. Measured and simulated results agree very well in almost the cabin area. Differences in peak levels are below 3dB. From this agreement, accuracies of measured values are clarified.

Fig.7 shows measured and calculated results in a x-y plane. Measured points are at crossing points of meshes. Separations of measured points are 20mm(≈λ/5). Measured data are stored in a Excel file. Contours of equal strengths are produced by a Excel file procedure. When comparing contours of measured and calculated results, regions of equal field strengths agree very well within 3dB differences. From this agreement, it is shown that accuracies of measured values and resolutions of locations are satisfactory in this measurement.

Fig.8 shows simulated electric field in a x-z plane in front of MSA. It is shown that there are standing waves along z axis, too. The radiated waves from front and rear windows are also observed.

B. *Vertical Polarization*

Fig.9 shows measured and calculated electric field strengths of vertical polarizations. It is remarkable that standing waves

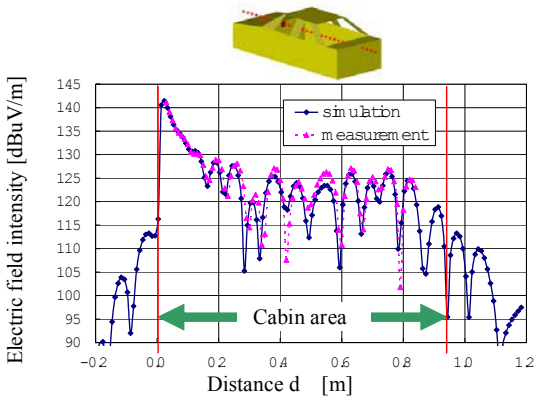

Fig .6: The electric field intensity in front of the MSA along X axis (horizontal polarization wave).

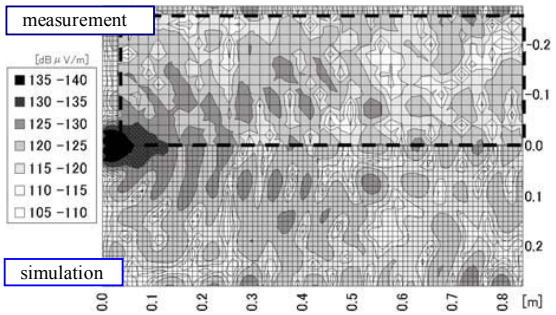

Fig .7: The electric field intensity in X-Y plane at the height of MSA (horizontal polarization wave).

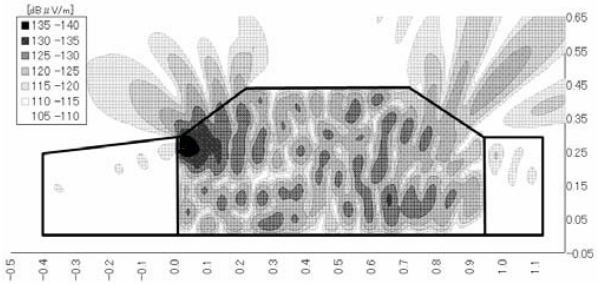

Fig .8: The simulated electric field intensity in X-Z plane in front of the MSA(horizontal polarization wave).

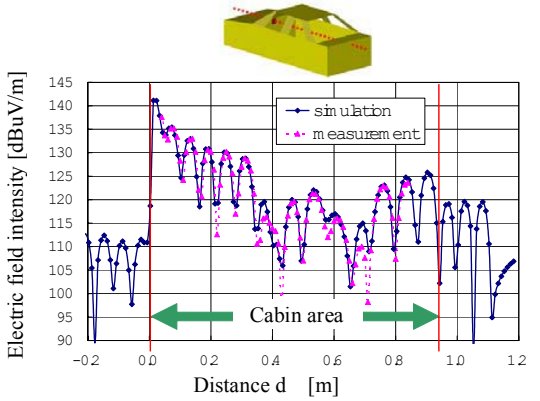

Fig .9: The electric field intensity in front of the MSA along X axis (vertical polarization wave).

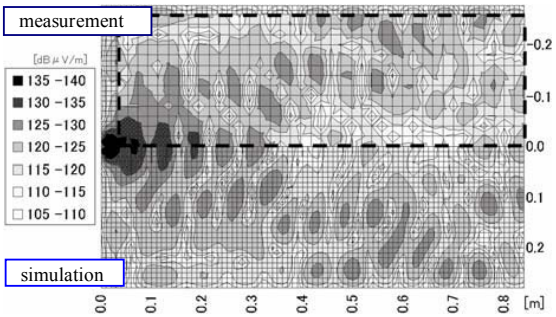

Fig .10: The electric field intensity in X-Y plane at the height of MSA (vertical polarization wave).

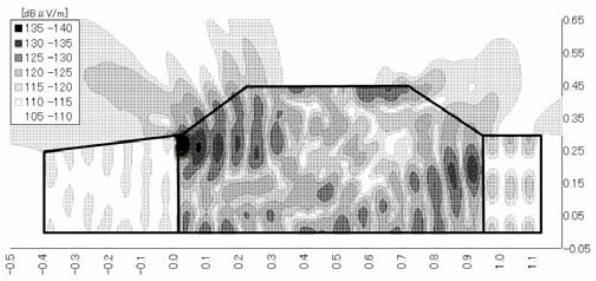

Fig .11: The simulated electric field intensity in X-Z plane in front of the MSA(vertical polarization wave).

are started at the face of the MSA. In a cabin area, these results agree very well. From this agreement, accuracies of measured values are ensured.

Fig.10 shows measured and calculated results in vertical polarizations. As in a horizontal polarization case, contours of equal field strengths agree very well. From this agreement, accuracies of measurements are also ensured.

Fig.11 shows simulated electric field in a x-z plane in front of MSA. It is shown that standing waves exist along z axis, too. Radiated waves from front and rear windows are also observed. Electrical fields at the middle of the cabin become lower about 5 dB than surrounding places. This is because the MSA is located at a weak point of standing waves. Detailed study will be made in the next sub section.

C. Standing Waves in a Car

Electric field distributions inside a car are considered affected strongly by the MSA position. Fig.12 (a),(b) shows calculated results at the MSA position that maximizes electrical field distributions. It is observed that standing wave shapes emerge clearly in a x-y plane. When comparing standing wave shapes of Fig.12(a),(b) and Fig.10,11, electrical field intensities inside a car are strongly affected by the MSA position. It is shown that Fig.10,11 are weak standing wave cases.

Standing wave numbers can be explained through a cavity model analysis. The cavity resonance frequency f_{lmn} is expressed by next equation.

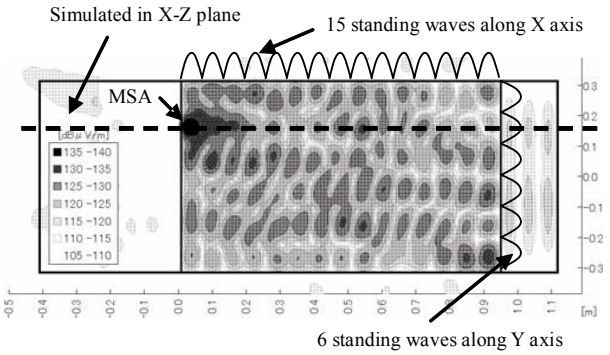

(a) x-y plane

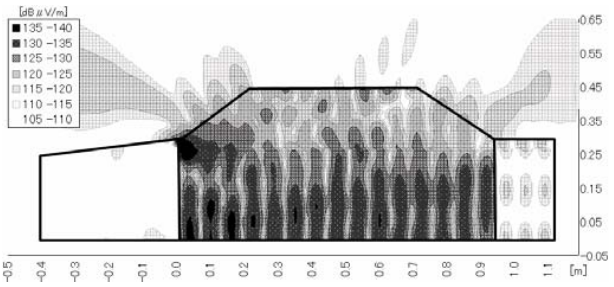

(b) x-z plane

Fig. 12: The simulated standing waves distributed in a car.

$$f_{lmn} = 3\times10^8 \times \sqrt{\left(\frac{l}{2a}\right)^2 + \left(\frac{m}{2b}\right)^2 + \left(\frac{n}{2h}\right)^2} \quad \cdots\cdots (2)$$

Here, a, b and h are length, width and height of the cabin, respectively. l, m and n are integers. In this case, a=940mm, b=579mm, and h=446mm are used. In Fig.12(a), standing waves along the x and y axes are 15 and 6, respectively. In Fig.12(b), electrical fields below the window become constant toward the z direction. This is because vertical polarizations have no traveling waves toward the z direction. In the upper part of the window, electrical field intensities become weak. This is considered due to radiations out side a car. As for the resonance frequency, by inserting l=15, m=6 and n=0 in Eq(2), f_{lmn} becomes 2854MHz. This calculated frequency is very close to the 2859MHz.

6. CONCLUSIONS

Electric fields in a scale-modelled-car are evaluated through measurements with an optical electric field probe and simulations. Measured and simulated electric fields in a car agreed very well within 3dB difference. From this agreement, it is shown that accuracies of measured values and resolutions of locations are sufficient in this measurement. It is ensured that electrical field measurements by an optical electric prove can provide precise results. It is also shown that distribution of standing waves in a cabin can be recognized through a cavity model analysis.

ACKNOWLEDGEMENT

The authors would like to express their sincere thanks to Dr. K. Hashimoto and Dr. S. Shimada of YTC for their continuous encouragement.

REFERENCES

[1] K.Fujimoto, "Overview of antenna systems for mobile communications and prospects for the future technology," IEICE Trans. Commun., vol.E74-B, no.10, pp.3191-3201, October 1991.

[2] S.Tanaka, S.Yuminaga and T.Kimura, "On-board multi-layered microstrip antenna and associated RF circuits for multiple ITS applications," Proc. 11th World Congress on Intelligent Transport Systems, IS01, No.3059, October 2004.

[3] M.Tanaka and Y.Miyazaki, "An Investigation of Radio Wave Intensity Distribution in the Automobile Body", IEICE Transactions, J69-B-12,pp.1804-1810,1986.

[4] K.Satou, K.Nishikawa, K.Matuhisa and N.Suzuki,"Analysis of Electric Field Distribution near Car body", Technical report of IEICE, AP97-89, August 1997.

[5] N.Nakakura, Y.Yamada, N.Michishita, "MoM simulations for Electrical Field Distributions of a Car ", Journal of the Japan Society for Simulation Technology,vol24 No 12,pp.45-52,June 2005.

[6] FEKO User's Manual Suite 5.0,EM Software & Systems,July 2005.